Inorg. Chem. **2005**, *44*, 7530–7539

Structure and Magnetic Properties of (*meso*-Tetraphenylporphinato)manganese(III) Bis(dithiolato)nickelates

Louise N. Dawe,[†] Jesse Miglioi,[†] Laura Turnbow,[†] Michelle L. Taliaferro,[†] William W. Shum,[†] Joshua D. Bagnato,[†] Lev N. Zakharov,[‡] Arnold L. Rheingold,[‡] Atta M. Arif,[†] Marc Fourmigué,[§] and Joel S. Miller*[,†]

Department of Chemistry, University of Utah, 315 S. 1400 East, RM 2020, Salt Lake City, Utah 84112-0850, Laboratoire Chimie Inorganique, Matériaux et Interfaces (CIMI), FRE 2447, CNRS-Université d'Angers, 49045 Angers, France, and Department of Chemistry, University of California, San Diego, 9500 Gilman Drive, La Jolla, California 92093

Received June 15, 2005

The crystal structures of [MnTPP]{Ni[$S_2C_2H(CN)]_2$} [MnTPP = (*meso*-tetraphenylporphinato)manganese(III)] and [MnTPP]{Ni[$S_2C_2(CN)_2]_2$} have been determined. These salts possess trans-μ-coordination of $S = 1/2$ {Ni[$S_2C_2H(CN)]_2$}$\bullet^-$ and {Ni[$S_2C_2(CN)_2]_2$}$\bullet^-$ to Mn(III) and form parallel 1-D coordination polymer chains exhibiting ν_{CN} at 2210 and 2200 and 2220 and 2212 cm^{-1}, respectively. The bis(dithiolato) monoanions are planar and bridge two cations with MnN distances of 2.339(16), and 2.394(3) Å, respectively, which are comparable to related MnN distances observed for [MnTPP][TCNE]·*x*(solvates). In addition, [MnTP′P]{Ni[$S_2C_2(CN)_2]_2$} {H_2TP′P = *meso*-tetrakis[3,5-di-*tert*-butyl-4-hydroxyphenyl)porphyrin] and [MnTP′P(OH_2)]{Ni[$S_2C_2(CN)_2]_2$} were prepared. The latter forms isolated paramagnetic ions. The room-temperature values of χT for 1-D [MnTPP]{Ni[$S_2C_2H(CN)]_2$}, [MnTPP]-{Ni[$S_2C_2(CN)_2]_2$}, and [MnTP′P]{Ni[$S_2C_2(CN)_2]_2$} are 2.55, 3.28, and 2.86 emu K/mol, respectively. Susceptibility (χ) measurements between 2 and 300 K reveal weak antiferromagnetic interactions with $\Theta = -5.9$ and –0.2 K for [MnTPP]{Ni[$S_2C_2H(CN)]_2$} and [MnTPP]{Ni[$S_2C_2(CN)_2]_2$}, respectively, and stronger antiferromagnetic coupling of –50 K for [MnTP′P]{Ni[$S_2C_2(CN)_2]_2$} from fits of $\chi(T)$ to the Curie–Weiss law. The 1-D intrachain coupling, J_{intra}, of [MnTPP]{Ni[$S_2C_2H(CN)]_2$} and [MnTPP]{Ni[$S_2C_2(CN)_2]_2$} was determined from modeling $\chi T(T)$ by the Seiden expression ($H = -2J\mathbf{S}_i\cdot\mathbf{S}_j$) with $J/k_B = -8.00$ K (–5.55 cm^{-1}; –0.65 meV) for [MnTPP]{Ni[$S_2C_2H(CN)]_2$}, J/k_B = –3.00 K (–2.08 cm^{-1}; –0.25 meV) for [MnTP′P]{Ni[$S_2C_2(CN)_2]_2$}, and $J/k_B = -122$ K (–85 cm^{-1}) for [MnTP′P]-{Ni[$S_2C_2(CN)_2]_2$}. These observed negative J_{intra}/k_B values are indicative of antiferromagnetic coupling. These materials order as ferrimagnets at 5.5, 2.3, and 8.0 K, for [MnTPP]{Ni[$S_2C_2H(CN)]_2$}, [MnTPP]{Ni[$S_2C_2(CN)_2]_2$}, and [MnTP′P]-{Ni[$S_2C_2(CN)_2]_2$}, respectively, based upon the temperature at which maximum in the 10 Hz $\chi'(T)$ data occurs. [MnTP′P]{Ni[$S_2C_2(CN)_2]_2$} has a coercivity of 17 700 Oe and remanent magnetizations of 7250 emu Oe/mol at 2 K and 17 Oe and 850 emu Oe/mol at 5 K; hence, upon cooling it goes from being a soft magnet to being a very hard magnet.

Introduction

The study of magnetically ordered molecule-based materials is a growing area of contemporary chemistry.[2−4] The first organic-containing molecule-based magnet, $[Fe(C_5Me_5)_2]^{\bullet+}$[TCNE]$^{\bullet-}$ (TCNE = tetracyanoethylene), and has an ordering temperature, T_c, of 4.8 K.[5] Improvements led to the discovery of V(TCNE)$_x$·*y*(solvent), the first room-temperature organic magnet ($T_c \sim 400$ K).[6] Later a family of metallomacrocycle-based magnets typified by [MnTPP][TCNE]·2PhMe (H_2TPP = *meso*-tetraphenylporphyrin) were discovered[3a,7] Subsequently, a wide range of manganese porphyrin compounds

* To whom correspondence should be addressed. E-mail: jsmiller@chem.utah.edu.
[†] University of Utah.
[‡] CNRS-Université d'Angers.
[§] University of California, San Diego.

(1) (a) Miller, J. S., Dougherty, D., Eds. Proceedings on the Conference on Ferromagnetic and High Spin Molecular Based Materials. *Mol. Cryst. Liq. Cryst.* **1989**, *176*. (b) Kahn, D., Gatteschi, J. S., Miller, F., Palacio, O., Eds. Proceedings on the Conference on Molecular Magnetic Materials. *NATO ARW Mol. Magn. Mater.* **1991**, *E198*. (c) Iwamura, H., Miller, J. S., Eds. Proceedings on the Conference on the Chemistry and Physics of Molecular Based Magnetic Materials. *Mol. Cryst. Liq. Cryst.* **1993**, *232/233*. (d) Miller, J. S., Epstein, A. J., Eds. Proceedings on the Conference on Molecule-Based Magnets. *Mol. Cryst. Liq. Cryst.* **1995**, *271−274*. (e) Itoh, K., Miller, J. S., Takui, T., Eds. Proceedings on the Conference on Molecular-Based Magnets. *Mol. Cryst. Liq. Cryst.* **1997**, *305/306*. (f) Turnbull, M. M., Sugimoto, T., Thompson, L. K., Eds. *ACS Symp. Ser.* **1996**, *No. 644*.

10.1021/ic050980u CCC: $30.25
Published on Web 09/14/2005

has been structurally characterized with [TCNE]$^{\bullet-}$ trans-μ-N-σ-bound to Mn^{III} forming a 1-D coordination polymer consisting of parallel chains of alternating $\cdots D^+A^{\bullet-}D^+A^{\bullet-}\cdots$ (D = MnTPP; A = radical anion).[3a] These materials are ferrimagnets resulting from the antiferromagnetic coupling of the $S = 2$ Mn^{III} with $S = 1/2$ [TCNE]$^{\bullet-}$ with critical temperatures, T_c, ranging from 3.5 to 28 K.[3a,8] Furthermore, at low temperature they exhibit complex magnetic behaviors that include large coercivities in the range of 27 kOe.[9] Herein, we extend the A$^{\bullet-}$ to bis(2-cyano-1,2-ethanedithiolato)-nickelate(III) (**1**) {Ni[S$_2$C$_2$H(CN)]$_2$}$^{\bullet-}$ [10] and (bis(maleonitrile)dithiolato)nickelate(III) (**2**) {Ni[S$_2$C$_2$(CN)$_2$]$_2$}$^{\bullet-}$.[11,12] **2** is of particular interest as it has been reported as [NH$_4$]**2**·H$_2$O to magnetically order as a weak ferromagnetic at 4.9 K.[13] Furthermore, while magnetic order has not been reported for metallocenium salts of **2**, they frequently exhibit ferromagnetic coupling[14] and decamethymanganocenium salts of {Ni[S$_2$C$_2$(CF$_3$)$_2$]$_2$}$^{\bullet-}$ order as metamagnets.[14,15] Herein, [MnTPP]{Ni[S$_2$C$_2$H(CN)]$_2$} and [MnTPP]{Ni[S$_2$C$_2$(CN)$_2$]$_2$} have been prepared and are reported. Additionally, due to the increased steric constraints of substitution of the phenyl rings in the 3,5-positions with *tert*-butyl groups, higher magnetic ordering temperatures have been observed;[16,17] hence, [MnTP′P]{Ni[S$_2$C$_2$(CN)$_2$]$_2$} (H$_2$TP′P = *meso*-tetrakis-(3,5-di-*tert*-butyl-4-hydroxyphenyl)porphyrin) was prepared and its magnetic properties compared to [MnTPP]{Ni[S$_2$C$_2$H-(CN)]$_2$} and [MnTPP]{Ni[S$_2$C$_2$(CN)$_2$]$_2$}.

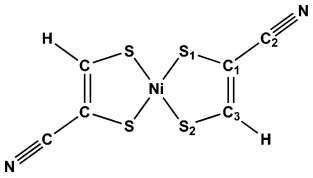

{Ni[S$_2$C$_2$H(CN)]$_2$}$^{\cdot-}$ (**1**)

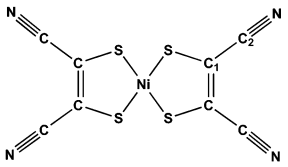

{Ni[S$_2$C$_2$(CN)$_2$]$_2$}$^{\cdot-}$ (**2**)

Experimental Section

Synthesis. Solvents for the preparation of manganese porphyrins were used as received. Solvents used for preparation of the electron-transfer salts were distilled under nitrogen from appropriate drying agents before use, and the syntheses of electron-transfer salts were carried out in inert atmosphere DriLab or using standard Schlenck vacuum techniques. TCNQF$_4$ was obtained as a gift from the Du Pont Co. and was recrystallized from CH$_2$Cl$_2$ prior to use. [NBu$_4$]-{Ni[S$_2$C$_2$(CN)$_2$]$_2$}[11b] and [HNMe$_3$]{Ni[S$_2$C$_2$H(CN)]$_2$}[10] were synthesized according to literature procedures. Pyrrole was dried by vacuum distillation from CaH$_2$.

All free-base porphyrins were prepared by the Adler−Longo method that involves refluxing pyrrole and the appropriately substituted benzaldehyde in propionic acid for 30 min.[18] Chlorin impurities were removed via the metalation of the corresponding free-base porphyrins. Relative purity was confirmed by thin-layer chromatography and/or UV−visible spectroscopy. The free-base porphyrins were metalated according to the literature[19] method by reaction with MnI$_2$ in dichloromethane stabilized with triethylamine. The products were purified via boiling in toluene to remove the triethylamine and then recrystallized from CH$_2$Cl$_2$/MeOH. MnTPP and MnTP′P were further purified by dynamic vacuum sublimation at 325 °C and 50 mTorr.

[MnTPP]{Ni[S$_2$C$_2$H(CN)]$_2$}, 3. Mn^{III}TPPCl (95.61 mg; 0.136 mmol) and Ag[SbF$_6$] (47.94 mg; 0.140 mmol) were dissolved in ∼7 mL of CH$_2$Cl$_2$ to give green and clear solutions, respectively. The Ag[SbF$_6$] solution was added dropwise to the rapidly stirred MnTPPCl solution to produce a black solution containing [Mn^{III}-TPP][SbF$_6$]. This solution was left to stir for an additional 30 min, and then it was filtered to remove AgCl. [HNMe$_3$]{Ni[S$_2$C$_2$H-(CN)]$_2$} (45.32 mg; 0.131 mmol) dissolved in ∼15 mL of CH$_2$Cl$_2$ was slowly diffused into the above filtrate using a three-compartment vessel. After 14 days the vessel was opened and X-ray-quality crystals and some purple powder were collected. IR (Nujol, ν_{CN}): 2210 (m), 2200 (s) cm^{-1}.

[MnTPP]{Ni[S$_2$C$_2$(CN)$_2$]$_2$}, 4. The above method was used except that [NBu$_4$]{Ni[S$_2$C$_2$(CN)$_2$]$_2$} was the anion. IR (Nujol, ν_{CN}): 2220 (m), 2212 (s) cm^{-1}.

(2) Reviews: (a) Miller, J. S.; Epstein, A. J. *Chem. Commun.* **1998**, 1319. (b) Ovcharenko, V. I.; Sagdeev, R. Z. *Russ. Chem. Rev.* **1999**, *68*, 345. (c) Plass, W. *Chem. Z.* **1998**, *32*, 323. (d) Miller, J. S.; Epstein, A. J. *Chem. Eng. News* **1995**, *73* (No. 40), 30. (e) Miller, J. S.; Epstein, A. J. *Angew. Chem., Int. Ed. Engl.* **1994**, *33*, 385. (f) Kinoshita, M. *Jpn. J. Appl. Phys.* **1994**, *33*, 5718. (g) Miller, J. S.; Epstein, A. J. *Adv. Chem. Ser.* **1995**, *245*, 161. (h) Caneschi, A.; Gatteschi, D. *Prog. Inorg. Chem.* **1991**, *37*, 331. (i) Buchachenko, A. L. *Russ. Chem. Rev.* **1990**, *59*, 307. (j) Kahn, O. *Struct. Bonding* **1987**, *68*, 89. (k) Caneschi, A.; Gatteschi, D.; Sessoli, R.; Rey, P. *Acc. Chem. Res.* **1989**, *22*, 392. (l) Gatteschi, D. *Adv. Mater.* **1994**, *6*, 635.

(3) Day, P. *Notes Rec. R. Soc. London* **2002**, *56*, 95. Miller, J. S. *Adv. Mater.* **2002**, *14*, 1105.

(4) Miller, J. S.; Calabrese, J. C.; Epstein, A. J.; Bigelow, R. W.; Zhang, J. H.; Reiff, W. M. *J. Chem. Soc., Chem. Commun.* **1986**, 1026. Miller, J. S.; Calabrese, J. C.; Rommelmann, H.; Chittipeddi, S.; Zhang, J. H.; Reiff, W. M.; Epstein, A. J. *J. Am. Chem. Soc.* **1987**, *109*, 769.

(5) (a) Manriquez, J. M.; Yee, G. T.; McLean, R. S.; Epstein, A. J.; Miller, J. S. *Science* **1991**, *252*, 1415. (b) Epstein, A. J.; Miller, J. S. In *Proceedings of Nobel Symposium #NS-81 Conjugated Polymers and Related Materials: The Interconnection of Chemical and Electronic Structure*; Oxford University Press: New York, 1993; p 475. Epstein, A. J.; Miller, J. S. *Chim. Ind.* **1993**, *75*, 185, 257. (c) Miller, J. S.; Yee, G. T.; Manriquez, J. M.; Epstein, A. J. In *Proceedings of Nobel Symposium #NS-81 Conjugated Polymers and Related Materials: The Interconnection of Chemical and Electronic Structure*; Oxford University Press: New York, 1993; p 461. Miller, J. S.; Yee, G. T.; Manriquez, J. M.; Epstein, A. J. *Chim. Ind.* **1992**, *74*, 845.

(6) (a) Miller, J. S.; Calabrese, J. C.; McLean, R. S.; Epstein, A. J. *Adv. Mater.* **1992**, *4*, 498. (b) Zhou, P.; Morin, B. G.; Epstein, A. J.; McLean, R. S.; Miller, J. S. *J. Appl. Phys.* **1993**, *73*, 6569. Brinckerhoff, W. B.; Morin, B. G.; Brandon, E. J.; Miller, J. S.; Epstein, A. J. *J. App. Phys.* **1996**, *79*, 6147.

(7) Rittenberg, D. K.; Miller, J. S. *Inorg. Chem.* **1999**, *38*, 4838.

(8) Rittenberg, D. K.; Sugiura, K-i.; Sakata, Y.; Mikami, S.; Epstein, A. J.; Miller, J. S. *Adv. Mater.* **2000**, *12*, 126.

(9) Fourmigué, M.; Bertran, J. N. *Chem. Commun.* **2000**, 2111.

(10) Gray, H. B.; Williams, R.; Bernal., I.; Billig, E. *J. Am. Chem. Soc.* **1962**, *84*, 3596. Davison, A.; Edelstein, N.; Holm, R. H. Maki, A. H. *J. Am. Chem. Soc.* **1963**, *85*, 2029. Davison, A.; Edelstein, N.; Holm, R. H. Maki, A. H. *Inorg. Chem.* **1963**, *2*, 1227. (b) Davison, A.; Holm, R. H. *Inorg. Synth.* **1967**, *10*, 8.

(11) Clemenson, P. I. *Coord. Chem. Rev.* **1990**, *106*, 71. Robertson, N.; Cronin, L. *Coord. Chem. Rev.* **2002**, *227*, 93.

(12) Coomber, A. T.; Deljonne, D.; Friend, R. H.; Bredas, J. L.; Charlton, A.; Robertson, N.; Underhill, A. E.; Kurmoo, M.; Day, P. *Nature* **1996**, *380*, 144.

(13) Yee, G. T.; Miller, J. S. In *Magnetism-Molecules to Materials*; Miller, J. S., Drillon, M., Eds.; Wiley-VCH: Mannheim, Germany, 2004; Vol. 5, p 223. Gama, V.; Durate, M. T. In *Magnetism-Molecules to Materials*; Miller, J. S., Drillon, M., Eds.; Wiley-VCH: Mannheim, Germany, 2004; Vol. 5, p 1.

(14) Broderick, W. E.; Thompson, J. A.; Hoffman, B. M. *Inorg. Chem.* **1991**, *30*, 2958.

(15) Böhm, A.; Vazquez, C.; McLean, R. S.; Calabrese, J. C.; Kalm, S. E.; Manson, J. L.; Epstein, A. J.; Miller, J. S. *Inorg. Chem.* **1996**, *35*, 3083.

(16) Brandon, E. J.; Kollmar, C.; Miller, J. S. *J. Am. Chem. Soc.* **1998**, *120*, 1822.

(17) Adler, A. D.; Longo, F. R.; Finarelli, J. D.; Goldmacher, J.; Assour, J.; Korsakoff, L. *J. Org. Chem.* **1967**, *32*, 476.

(18) Lindsey, J. S.; Woodford, J. N. *Inorg. Chem.* **1995**, *34*, 1063.

(19) Brandon, E. J.; Rittenberg, D. K.; Arif, A. M.; Miller, J. S. *Inorg. Chem.* **1998**, *37*, 3376.

Table 1. Summary of the Crystallographic Data for [MnTPP]{Ni[$S_2C_2H(CN)]_2$}, **3**, [MnTPP]{Ni[$S_2C_2(CN)_2]_2$}, **4**, and [MnTP′P(OH_2)]{Ni[$S_2C_2(CN)_2]_2$}·EtOH·H_2O, **6**

param	[MnTPP]{Ni[$S_2C_2H(CN)]_2$}, **3**	[MnTPP]{Ni[$S_2C_2(CN)_2]_2$}, **4**	[MnT′PP(OH_2)]{Ni[$S_2C_2(CN)_2]_2$}·EtOH·H_2O, **6**
formula	$C_{50}H_{30}MnN_6NiS_4$	$C_{52}H_{28}MnN_8NiS_4$	$C_{86}H_{102}MnN_8NiO_7S_4$
formula mass	956.69	1006.71	1601.65
space group	$P\bar{1}$	$P\bar{1}$	$P\bar{1}$
a, Å	10.6560(3)	10.4769(9)	14.647(3)
b, Å	10.7154(4)	10.8561(9)	16.688(3)
c, Å	10.8898(2)	11.2213(9)	19.783(4)
α, deg	97.8288(18)	99.060(2)	90.842(3)
β, deg	117.3550(16)	101.452(2)	98.920(3)
γ, deg	98.5935(15)	113.5120(10)	113.425(3)
Z	1	1	2
V, $Å^3$	1061.86(5)	1106.54(16)	4367.8(15)
μ, cm^{-1}	0.982	0.948	0.511
ρ_{calcd}, g/cm^3	1.496	1.511	1.218
$R(F)^a$	0.0411	0.0435	0.0756
$wR(F^2)^b$	0.0768	0.1092	0.1522
T, K	150(1)	218(2)	100(2)
λ, Å	0.710 73	0.710 73	0.710 73

[a] $R(F) = \Sigma(|F_o| - |F_c|)/\Sigma|F_o|$. [b] $wR(F^2) = [\Sigma(w(F_o^2 - F_c^2)^2)/\Sigma(F_o^2)^2]^{1/2}$.

[MnTP′P]{Ni[$S_2C_2(CN)_2]_2$}, 5. The above method for **4** was used except that MnTP′PCl was utilized and [Mn^{III}TP′P][SbF_6] was prepared in situ. IR (Nujol, ν_{CN}): 2208 (s) cm^{-1}. Anal. Calcd (obsd) for $C_{84}H_{92}MnN_4NiS_4$: C, 66.39 (66.42); H, 6.10 (6.15); N, 7.37 (7.51). TGA analysis of **5** reveals that it is thermally stable below 260 °C and decomposes at higher temperature. **5** forms very fine fibrous crystals that have precluded their structural study. Nonetheless, crystals of [MnTP′P(OH_2)]{Ni[$S_2C_2(CN)_2]_2$}·EtOH·H_2O, **6**, composition have been grown from ethanol/water.

Physical Methods. The thermal properties were studied on a TA Instruments model 2050 thermogravimetric analyzer (TGA) equipped with a TA-MS Fison triple filter quadrupole mass spectrometer, to identify gaseous products with masses less than 300 amu. This instrument is located in a Vacuum Atmospheres DriLab under argon to protect air- and moisture-sensitive samples. Samples were placed in an aluminum pan and heated at 20 °C/min under a continuous 10 mL/min nitrogen flow. The 2−300 K magnetic susceptibility was determined on a Quantum Design MPMS-5XL 5 T SQUID (sensitivity = 10^{-8} emu or 10^{-12} emu/Oe at 1 T) or a PPMS 9T as previously described.[20] Due to the large diamagnetic component of the observed magnetization, all magnetic measurements were perform in closed nonairtight gelatin capsules. In addition to correction for the diamagnetic contribution from the sample holder, core diamagnetic corrections of -430×10^{-6}, -804×10^{-6}, -82×10^{-6}, and -91×10^{-6} emu/mol based on summing Pascal's constants were used for MnTPP, MnTP′P, {Ni[$S_2C_2H(CN)]_2$}$^{\bullet-}$, and {Ni[$S_2C_2(CN)_2]_2$}$^{\bullet-}$, respectively. Infrared spectra ((600−4000) ± 1 cm^{-1}) were obtained on a Bruker Tensor 37 FT IR-40 spectrophotometer as potassium bromide pellets. Elemental analyses were performed by Complete Analysis Laboratories Inc. of Parsippany, NJ.

Ab initio calculations were executed using the hybrid B3LYP exchange and correlation DFT[21] with the 6-31++g(d,p) basis set.[22] All calculations were done using Gaussian-03.[23] The optimized structures of **1** and 2 were based on the reported crystal structure for [NEt_4]**1**.[24] Trans-substitution of H for CN onto the optimized structure of **2** yielded **1**. Each radical anion was optimized completely. Mulliken and natural bond orbital (NBO) charge and spin distributions were calculated.[25] NBO spin densities were determined for both α and *β* electron populations for each unique atoms within **2** and **1**. The spin density was calculated from the differences between the α and the *β* electron populations.[26]

X-ray Structure Determination. Single crystals of **3**, **4**, and **6** were grown from their respective solvents via slow diffusion, and their unit cells were determined on a Nonius KappaCCD diffractometer equipped with Mo Kα radiation. The crystallographic data are summarized in Table 1. Equivalent reflections were merged, and only those for which $I_o > 2\sigma(I)$ were included in the refinement, where $\sigma(F_o)^2$ is the standard deviation based on counting statistics. Reflections were indexed, integrated, and corrected for Lorentz, polarization, and absorption effects using DENZO-SMN and SCALEPAC.[27] The structure was solved by a combination of direct methods and heavy atom methods using SIR 97.[28] All of the nonhydrogen atoms were refined with anisotropic displacement coefficients. Hydrogen atoms were assigned isotropic displacement coefficients $U(H) = 1.2U(C)$, and their coordinates were allowed to ride on their respective carbons using SHELXL97.[29]

(20) The B3LYP is a combination of the nonlocal three-parameter exchange functional (Becke, A. D. *J. Chem. Phys.* **1993**, *98*, 5648) and nonlocal LYP correlation functional (Lee, C.; Yang, W.; Parr, R. G. *Phys. Rev. B* **1998**, *37*, 785).

(21) (a) Ditchfield, R.; Hehre, W. J.; Pople, J. A. *J. Chem. Phys.* **1971**, *54*, 724. (b) Clark, T.; Chandrasekhar, J.; Spitznagel, G. W.; Schleyer, R. v. R. *J. Comput. Chem.* **1983**, *4*, 294.

(22) Frisch, M. J.; Trucks, G. W.; Schlegel, H. B.; Scuseria, G. E.; Robb, M. A.; Cheeseman, J. R.; Montgomery, J. A., Jr.; Vreven, T.; Kudin, K. N.; Burant, J. C.; Millam, J. M.; Iyenger, S. S.; Tomasi, J.; Barone, V.; Mennucci, B.; Cossi, M.; Scalmani, G.; Rega, N.; Petersson, G. A.; Nakatsuji, H.; Hada, M.; Ehara, M.; Toyota, K.; Fukuda, R.; Hasegawa, J.; Ishida, M.; Nakajima, T.; Honda, Y.; Kitao, O.; Nakai, H.; Klene, M.; Li, X.; Knox, J. E.; Hratchian, H. P.; Cross, J. B.; Adamo, C.; Jaramillo, J.; Gomperts, R.; Stratmann, R. E.; Yazyev, O.; Austin, A. J.; Cammi, R.; Pomelli, C.; Ochterski, J. W.; Ayala, P. Y.; Morokuma, K.; Voth, G. A.; Salvador, P.; Dannenberg, J. J.; Zakrewski, V. G.; Dapprich, S.; Daniels, A. D.; Strain, M. C.; Farkas, O.; Malick, D. K.; Rabuck, A. D.; Raghavachari, K.; Foreman, J. B.; Ortiz, J. V.; Cui, Q.; Baboul, A. G.; Clifford, S.; Cioslowski, J.; Stefanov, B. B.; Liu, G.; Liashenko, A.; Piskorz, P.; Komaromi, I.; Martin, R. L.; Fox, D. J.; Keith, T.; Al-Laham, M. A.; Peng, C. Y.; Nanayakkara, A.; Challacombe, M.; Gill, P. M. W.; Johnson, B.; Chen, W.; Wong, M. W.; Gonzalez, C.; Pople, J. A. *Gaussian 03*, revision B.02; Gaussian, Inc.: Pittsburgh, PA, 2003.

(23) Kobayahi, A.; Sasaki, Y. *Bull. Chem. Soc. Jpn.* **1977**, *50*, 2650.

(24) Glendening, E. D.; Reed, A. E.; Carpenter, A. E.; Weinhold, F. *NBO*, version 3.1.

(25) Szabo, A.; Ostlund, N. S. *Modern Quantum Chemistry: Introduction to Advanced Electronic Structure Theory*; Macmillan Publishing Co., Inc.: New York, 1982.

(26) Otwinowski, Z.; Minor, W. *Methods Enzymol.* **1997**, *276*, 307.

(27) Altomare, A.; Burla, M. C.; Camalli, M.; Cascarano, G.; Giacovazzo, C.; Guagliardi, A.; Moliteni, A. G. G.; Polidori, G.; Spagna, R. *SIR97-A program for automatic solution and refinement of crystal structure*, release 1.02.

(28) Sheldrick, G. M. *SHELX97 (Includes SHELXS97, SHELXL97, CIFTAB) Programs for Crystal Structure Analysis*, release 97-2; University of Göttingen: Göttingen, Germany, 1997.

The final cycle of full-matrix least-squares refinement of **3** was based on 7757 observed reflections [$I_o > 2\sigma(I)$] and converged with unweighted and weighted agreement factors R(F) = 0.0322 and wR(F^2) = 0.0710, respectively. The final cycle of full-matrix least-squares refinement of **4** was based on 8087 observed reflections [$I_o > 2\sigma(I)$] and converged with unweighted and weighted agreement factors R(F) = 0.0435 and wR(F^2) = 0.1092, respectively. The cations lie on crystallographic inversion centers with Mn at the center for both **3** and **4**.

An extremely thin lavender plate (0.41 × 0.31 × 0.004 mm) of **6** was mounted on a Cryo-loop. The structure was solved by direct methods. All non-hydrogen atoms were refined anisotropically, and hydrogen atoms were treated as idealized contributions. The final cycle of full-matrix least-squares refinement of **6** was based on 7075 observed reflections [$I_o > 2\sigma(I)$] and converged with unweighted and weighted agreement factors R(F) = 0.0756 and wR(F^2) = 0.1522, respectively. The asymmetric unit consists of $[Mn^{III}TP'P(OH_2)]^+$, two half-$\{Ni[S_2C_2(CN)_2]_2\}^-$ anions located on inversion centers, and one molecule of water and one molecule of EtOH of solvation.

Results and Discussion

Synthesis. Magnetically ordered [MnTPP][TCNE] are prepared via the electron-transfer reaction of Mn^{II}TPP and TCNE, eq 1. However, neither $\{Ni[S_2C_2(CN)_2]_2\}^0$ nor $\{Ni[S_2C_2(CN)_2]_2\}^0$ is stable; hence, eq 1 using these acceptors is not an option. The sequential oxidation of Mn^{II}TPP with $Ag[SbF_6]$ forming $[Mn^{III}TPP][SbF_6]$ in situ and the metathesis reaction with either $\{Ni[S_2C_2H(CN)]_2\}^{\bullet-}$ or $\{Ni[S_2C_2(CN)_2]_2\}^{\bullet-}$, eq 2, forming $[Mn^{III}TPP]\{Ni[S_2C_2H(CN)]_2\}$ or $[Mn^{III}TPP]$, respectively, was utilized.

$$Mn^{II}TPP + TCNE \rightarrow [Mn^{III}TPP]^+[TCNE]^{\bullet-} \quad (1)$$

$$Mn^{II}TPP + Ag^+ \rightarrow [Mn^{III}TPP]^+ \quad (2a)$$

$$[Mn^{III}TPP]^+ + \{Ni[S_2C_2(CN)_2]_2\}^{\bullet-} \rightarrow [Mn^{III}TPP]\{Ni[S_2C_2(CN)_2]_2\} \quad (2b)$$

Since $\{Ni[S_2C_2H(CN)]_2\}^{\bullet-}$ [$E_{1/2}° = -0.31$ V vs SCE][10] and $\{Ni[S_2C_2(CN)_2]_2\}^{\bullet-}$ [$E_{1/2}° = 0.23$ V][10] are easily reduced to the dianion, care was extended to minimize their formation, but they are observed. X-ray-quality crystals were grown from solutions of CH_2Cl_2 by slow diffusion. Unexpectedly, neither $[Mn^{III}TPP]\{Ni[S_2C_2H(CN)_2]\}$ nor $[Mn^{III}TPP]\{Ni[S_2C_2(CN)_2]_2\}$ is solvated as observed for all previously characterized TCNE electron-transfer salts with MnTPP or substituted MnTPP's[3a] as well as so many other MTPPs that they have been called sponges.[30] This eliminates differences in data arising from differing solvent contents.

Structural studies on **3** and **4** revealed that the μ-radical anion acceptor is nearly perpendicular with respect to the MnN_4 porphyrin plane (vide infra). The motif has been correlated to poor intrachain antiferromagnetic coupling and low magnetic ordering temperatures,[17] as were subsequently observed (vide infra). Hence, we targeted the preparation of $[MnTP'P]\{Ni[S_2C_2(CN)_2]_2\}$ (**5**) ($H_2TP'P$ = *meso*-tetrakis[3,5-di-*tert*-butyl-4-hydroxyphenyl)porphyrin], which due to the increased steric constraints arising from the substitution of the phenyl rings in the 3,5-positions with *tert*-butyl groups reduces the dihedral angle between the mean TCNE and MnN_4 planes and stronger antiferromagnetic coupling and higher magnetic ordering temperatures are expected as observed for [MnTP'P][TCNE].[16]

The shift of the ν_{CN} absorption of **3** (2210 and 2000 cm^{-1}), **4** (2220 and 2212 cm^{-1}), and **5** (2208 cm^{-1}) with respect to $[HNMe_3]\{Ni[S_2C_2H(CN)]_2\}$ (ν_{CN} = 2203 cm^{-1}) and $[NBu_4]\{Ni[S_2C_2(CN)_2]_2\}$ (ν_{CN} = 2206 cm^{-1}) indicates trans-μ-bonding of the dithiolate radical anion.

Structure. The structures of **3** and **4** were determined by single-crystal X-ray diffraction. The unit cell and metric parameters are summarized in Table 1, and the ORTEP drawings are presented in Figures 1 and 2. In each case the structures of the $[Mn^{III}TPP]^+$ cations, which lie on crystallographic inversion centers at Mn, are nearly indistinguishable and consistent with other D_{4h} $[Mn^{III}(por)]^+$ cations reported in the literature.[8,31,32] The TPP ligand is planar with Mn−N(pyrrole) bond distances averaging 2.005 Å. The bond distances and angles of the porphyrin ring are identical within the limits of the standard deviation for $[Mn^{III}(por)]^+$.

(29) (a) Goldberg, I.; Krupitsky, H.; Stein, Z.; Hsiou, Y.; Strouse, C. E. *Supramol. Chem* **1995**, *4*, 203. (b) Krupitsky, H.; Stein, Z.; Goldberg, I. *J. Inclusion Phenom. Mol. Recognit. Chem.* **1995**, *20*, 211. (c) Goldberg, I. *Mol. Cryst. Liq. Cryst*. **1996**, *278*, 767. (d) Byrn, M. P.; Curtis, C. J.; Hsiou, Y.; Kahn, S. I.; Sawin, P. A.; Tendick, S. K.; Terzis, A.; Strouse, C. E. *J. Am. Chem. Soc*. **1993**, *115*, 9480. Byrn, M. P.; Curtis, C. J.; Hsiou, Y.; Khan, S. I.; Sawin, P. A.; Terzis, A.; Strouse, C. E. In *Comprehensive Supramolecular Chemistry*; Atwood, J. L., Davies, J. E. D., MacNicol, D. D., Vogtle, F., Eds.; 1996; Vol. 6, p 715.

(30) (a) McKee, V.; Ong, C. C.; Rodley, G. A. *Inorg. Chem*. **1984**, *23*, 4242. (b) Barkigia, K. M.; Spaulding, L. D.; Fajer, J. *Inorg. Chem*. **1983**, *22*, 349.

(31) (a) Hibbs, W.; Rittenberg, D. K.; Sugiura, K.-i.; Burkhart, B. M.; Morin, B. G.; Arif, A. M.; Liable-Sands, L.; Rheingold, A. L.; Sundaralingam, M.; Epstein, A. J.; Miller, J. S. *Inorg. Chem.* **2001**, *40*, 1915. (b) Miller, J. S.; Epstein, A. J. *Chem. Commun.* **1998**, 1319. (c) Goldberg, I.; Krupitsky, H.; Stein, Z.; Hsiou, Y.; Strouse, C. E. *Supramol. Chem* **1995**, *4*, 203. (d) Krupitsky, H.; Stein, Z.; Goldberg, I. *J. Inclusion Phenom. Mol. Recognit. Chem.* **1995**, *20*, 211. (e) Goldberg, I. *Mol. Cryst. Liq. Cryst.* **1996**, *278*, 767. (f) Byrn, M. P.; Curtis, C. J.; Hsiou, Y.; Kahn, S. I.; Sawin, P. A.; Tendick, S. K.; Terzis, A.; Strouse, C. E. *J. Am. Chem. Soc*. **1993**, *115*, 9480. (g) Rittenberg, D. K.; Sugiura, K.-i..; Sakata, Y.; Mikami, S.; Epstein, A. J.; Miller, J. S. *Adv. Mater*. **2000**, *12*, 126. (h) Rittenberg, D. K.; Sugiura, K.-i..; Sakata, Y.; Guzei, I. A.; Rheingold, A. L.; Miller, J. S. *Chem.*—Eur. J. **1999**, *5*, 1874. (i) Sugiura, K.-i.; Arif, A.; Rittenberg, D. K.; Schweizer, J.; Öhrstrom, L.; Epstein, A. J.; Miller, J. S. *Chem.*—Eur. J. **1997**, *3*, 138. (j) Brandon, E. J.; Sugiura, K.-i.; Arif, A. M.; Liable-Sands, A.; Rheingold, A. L.; Miller, J. S. *Mol. Cryst., Liq. Cryst.* **1997**, *305*, 269. (k) Brandon, E. J.; Burkhart, B. M.; Rogers, R. D.; Miller, J. S. *Chem.*—Eur. J. **1998**, *4*, 1938. (l) Brandon, E. J.; Arif, A. M.; Burkhart, B. M.; Miller, J. S. *Inorg. Chem.* **1998**, *37*, 2792. (m) Brandon, E. J.; Arif, A. M.; Miller, J. S.; Sugiura, K.-i.; Burkhart, B. M. *Cryst. Eng*. **1998**, *1*, 97. (n) Sugiura, K.-i.; Mikami, S.; Tanaka, T.; Sawada, M.; Manson, J. L.; Miller, J. S.; Sakata, Y. *Chem. Lett*. **1997**, 1071. (o) Day, V. W.; Sults, B. R.; Tasset, E. L.; Marianelli, R. S.; Boucher, L. J. *Inorg. Nucl. Chem. Lett*. **1975**, *11*, 505. (p) Cheng, B.; Cukiernik, F.; Fries, P.; Marchon, J.-C.; Scheidt, W. R. *Inorg. Chem.* **1995**, *34*, 4627. (q) Guildard, R.; Perie, K.; Barbe, J.-M.; Nurco, D. J.; Smith, K. M.; Caemelbecke, E. V.; Kadish, K. M. *Inorg. Chem.* **1998**, *37*, 973. (r) Landrum, J. T.; Hatano, K.; Scheidt, W. R.; Reed, C. A. *J. Am. Chem. Soc.* **1980**, *102*, 6729. (s) Hill, C. L.; Williamson, M. M. *Inorg. Chem.* **1985**, *24*, 3024. (t) Fleischer, E. B. *Acc. Chem Res.* **1970**, *3*, 105. (u) Scheidt, W. R.; Reed, C. A. *Chem. Rev.* **1981**, *81*, 543. (v) Turner, P.; Gunter, M. J.; Hambley, T. W.; White, A. H.; Skelton, B. W. *Inorg. Chem.* **1992**, *31*, 2297.

(32) Zurcher, S.; Gramlich, V.; Arx, D. v.; Tongi, A. *Inorg. Chem.* **1998**, *37*, 4015. Day, M. W.; Qin, J.; Yang, C. *Acta Crystallogr*. **1998**, *C54*, 1413. Hobi, M.; Zurcher, S.; Gramlich, V.; Burckhardt, U.; Mensing, C.; Spahr, M.; Tongi, A. *Organometellics* **1996**, *15*, 5342. Brunn, K.; Endes, H.; Weiss, J. *Z. Naturforsh.* **1987**, *42b*, 1222. Ramakrishna, B. L.; Manoharan, P. T. *Inorg. Chem.* **1983**, *22*, 2213.

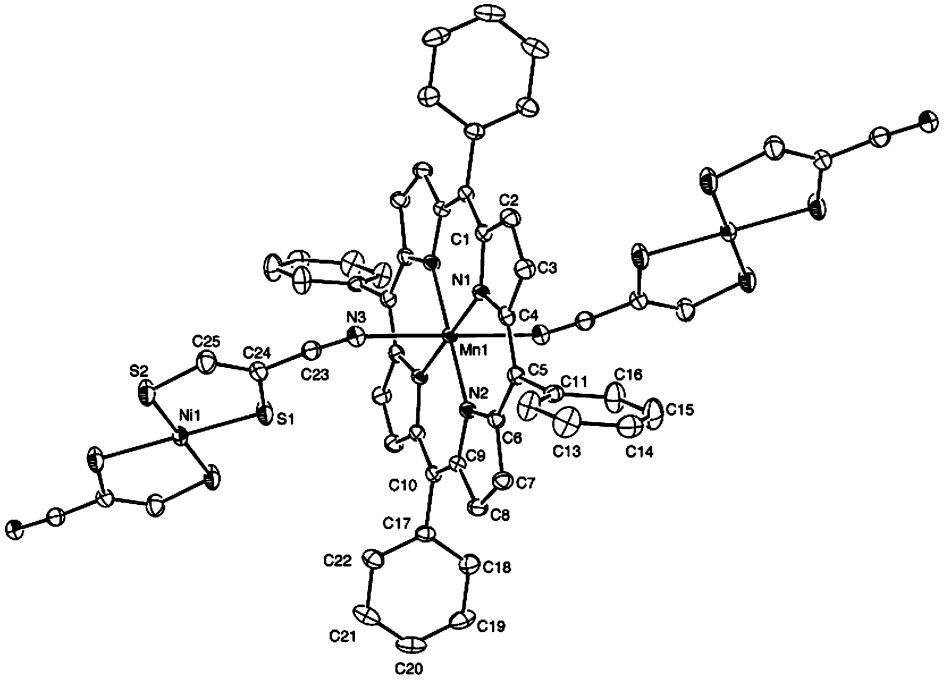

Figure 1. ORTEP atom-labeling diagram of [MnTPP]{Ni[$S_2C_2H(CN)]_2$}, **3**, using 30% thermal ellipsoids.

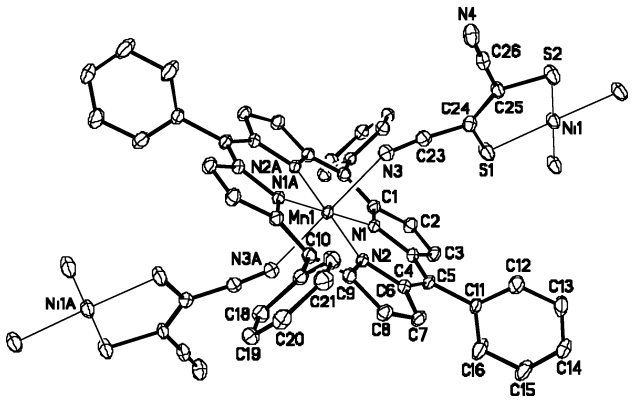

Figure 2. ORTEP atom-labeling diagram of [MnTPP]{Ni[$S_2C_2(CN)_2]_2$}, **4**, complexes using 30% thermal ellipsoids.

1[10] and **2**[33] are planar with intramolecular distances and angles comparable to that reported for the isolated ligands. **1** and **2** are uniformly trans-μ-N-σ-bound to two Mn^{III}'s forming parallel 1-D···$D^+A^{\bullet-}D^+A^{\bullet-}$··· [D = MnTPP; A = **1** (Figure 3) or **2** (Figure 4)] chains. Chains **I**−**II** and **I**−**III** are out-of-registry, and chains **II**−**II** and **I**−**IV** are in-registry. The key inter- and intrachain interaction can be found in Figures 3 and 4 and summarized in Table 2.

The acceptor N−Mn distances are 2.339(16) and 2.394(3) Å for **3** and **4**, respectively, which are on the high side but comparable to that observed for [MnTPP][TCNE]·*x*(solvates).[32a] The MnNC angles are 139.9 ± 1.5° while the dihedral angle between the mean MnN_4 and the mean acceptor planes range from 79.5 to 85.2° for **3** and **4**, respectively. These former values are typical of related compounds,[32] while the latter are on the high side indicative of poorer $p_z-d_{z^2}$ overlap and reduced coupling leading to lower T_c's.[17]

The intrachain Mn···Mn separations range from 14.20 to 14.33 Å for **3** and **4**, respectively, which are expectedly longer (>2 Å) than even the longest one observed (10.39 Å) for a member of the [MnTPP][TCNE]·*x*(solvates) family[34] as both **1** and **2** are much larger than $[TCNE]^{\bullet-}$. The larger Mn···Mn separations enable adjacent chains to interdigitate (Figures 3a and 4a) not enabling the solvent to be occluded. The out-of-registry interchain separations are 8.14 and 8.40 Å for **3** and **4**, respectively. This is at variance with all other [MTPPs][TCNE] that occlude solvents and are termed sponges.[30] The longer intra-N···N separation of 11 Å for **3** and **4** vs ~5.9 Å for $[TCNE]^{\bullet-}$ increases the intrachain Mn·· ·Mn separation by 45% to ~14.25 Å from ~9.8 Å enabling interdigitation to occur. $[TCNQF_4]^{\bullet-}$ with its N···N separation of ~9.5 Å (Mn···Mn separation = 12.68 Å), like $[TCNE]^{\bullet-}$, is also solvated.[35] This, it appears that Mn···Mn separations ~14 Å (and N···N separations ~10 Å) are needed for interdigitation to occur for the MnTPP family of 1-D coordination polymers.

Attempts to grow crystals of **5** suitable for a single-crystal X-ray structural analyses were unsuccessful due to formation of only fibrous needle crystals. Due to the stability of the $\mathbf{2}^{\bullet-}$, crystallization from ethanol/water was successful. However, the sought 1-D coordination polymer motif was not observed as the no terminal nitrogens $\{Ni[S_2C_2(CN)_2]_2\}^{\bullet-}$ bond to a Mn(III). Each Mn(III) is five coordinate with four N atoms and the axial water, and the unit cell has an ethanol and additional water molecule. The coordinated water and lattice water are H-bonded (O···O = 2.82 Å), and the molecule of EtOH is H-bonded to N5 in one of the Ni complexes. The Mn···S is 3.4 Å, which is less than the sum of the van der Waal radii indicative of an interaction. Hence, the composition is [MnTP′P(OH_2)]{Ni[$S_2C_2(CN)_2]_2$}·EtOH·

(33) Rittenberg, D. K.; Arif, A. M.; Miller, J. S. *J. Chem. Soc., Dalton Trans.* **2000**, 3939.
(34) Johnson, M. T.; Arif, A. M.; J. S. Miller, J. S. *Eur. J. Inorg. Chem.* **2000**, 1781.
(35) Values less than the calculated spin only value of 2.45 μ_B are attributed to weighing errors due to errors in molecular weight due to the specific degree of solvation and subtraction of the ferromagnetic impurity.

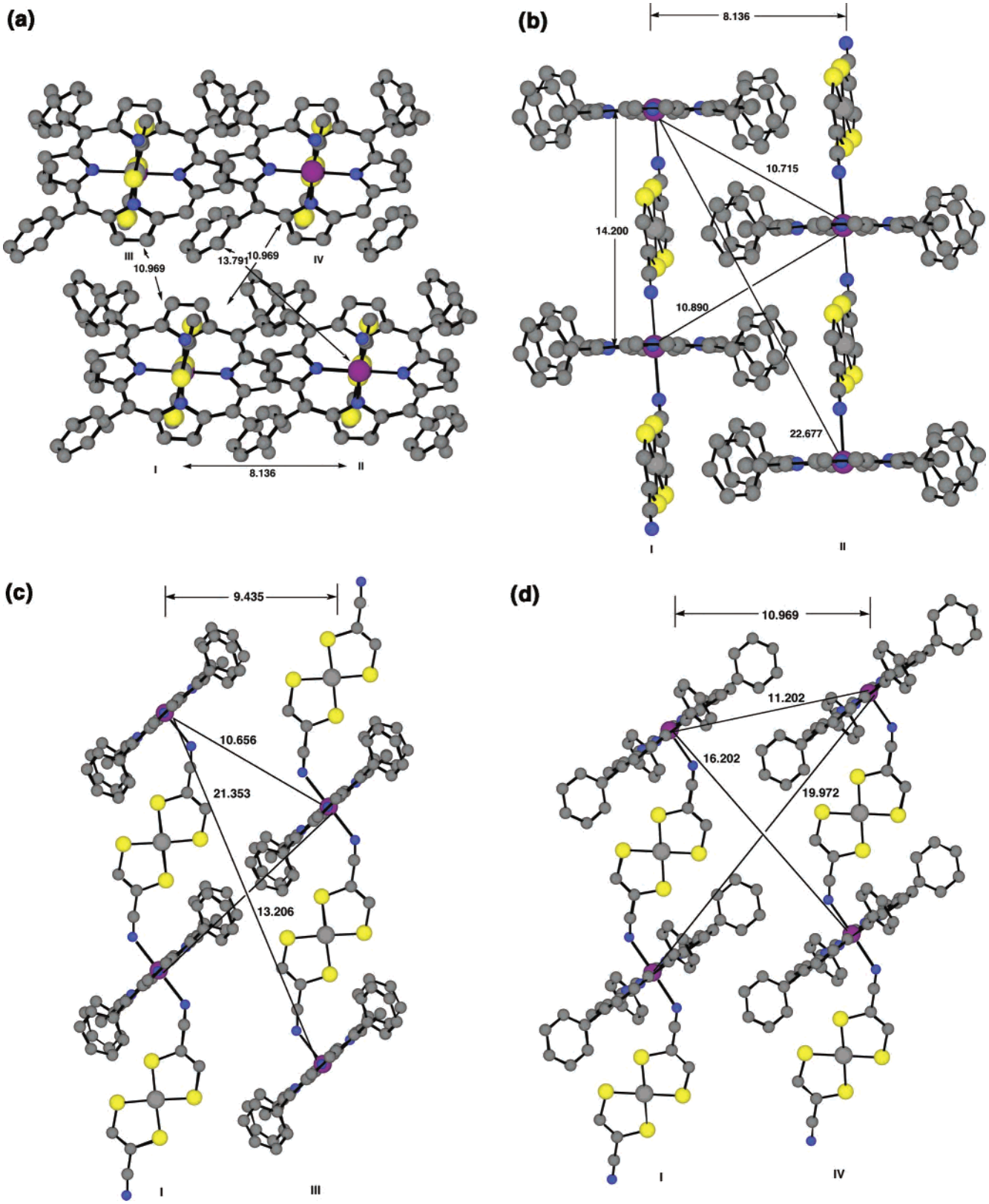

Figure 3. View down the *a*-axis normal to the parallel chains showing the interchain interactions among chains **I**−**IV** (a). View parallel to out-of-registry chains **I**−**II** (b) and **I**−**III** (c) and in-registry chains **I**−**IV** (s) and **II**−**III** (e) for [MnTPP]{Ni[$S_2C_2H(CN)]_2$}, **3**.

H_2O, **6**. The unit cell and metric parameters are summarized in Table 1, and the ORTEP atom labeling drawing is presented in Figure 5. The structures of the C_{4v} [Mn^{III}TPP-$(OH_2)]^+$ cation are nearly indistinguishable and consistent with related five coordinate $[Mn^{III}(por)]^+$ cations reported in the literature.

Magnetic Data. The 2−300 K corrected molar magnetic susceptibility, χ, was measured for **3**−**5**. The 300 K values

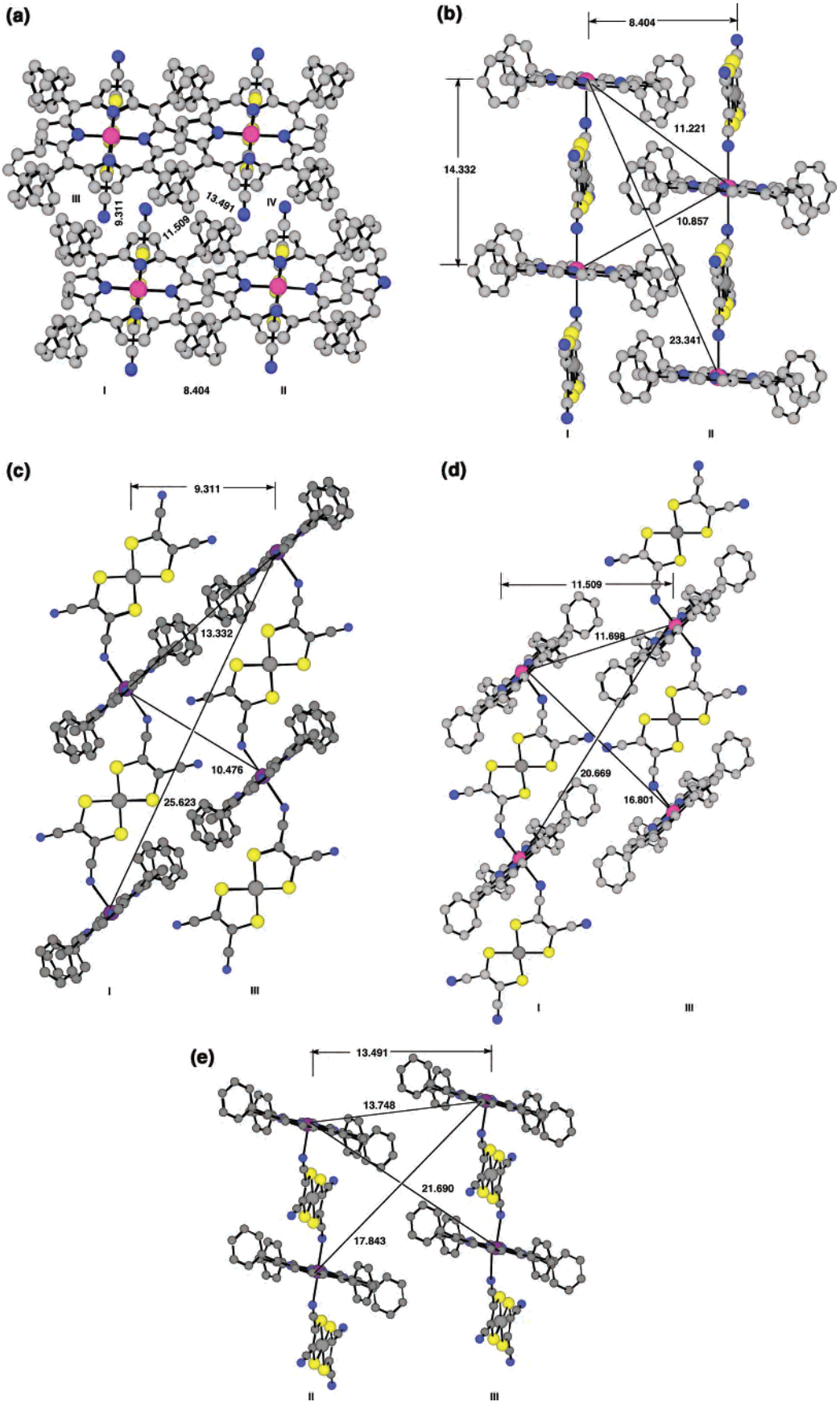

Figure 4. View down the *a*-axis normal to the parallel chains showing the interchain interactions among chains **I**−**IV** (a). View parallel to out-of-registry chains **I**−**II** (b) and **I**−**III** (c) and in-registry chains **I**−**IV** (d) and **II**−**III** (e) for [MnTPP]{Ni[$S_2C_2(CN)_2]_2$}, **4**.

Table 2. Summary of Key Bond Distances and Separations for [MnTPP]{Ni[S$_2$C$_2$H(CN)]$_2$}, **3**, and [MnTPP]{Ni[S$_2$C$_2$(CN)$_2$]$_2$}, **4**

param	[MnTPP]{Ni-[S$_2$C$_2$H(CN)]$_2$}, **3**	[MnTPP]{Ni-[S$_2$C$_2$(CN)$_2$]$_2$}, **4**
MnN_{CN}, Å	2.3390(16)	2.394(3)
MnNC, deg	139.39(15)	141.41(3)
MnN_4−TCNE dihedral angle, deg	79.5	85.2
MnN_{por}, Å	2.0072(15)	1.996(2)
	2.0140(14)	2.002(2)
N_{CN}−Mn−N_{CN}, deg	180.00(7)	180.00(12)
Mn···Mn intrachain, Å	14.200	14.332
Mn···Mn interchain,[a] Å	10.656[b]	10.476[b]
	10.715[b]	10.857[b]
	10.890[b]	11.221[b]
	11.202[c]	11.698[c]
	13.206[b]	13.332[b]
	13.937[c]	13.748[c]
interchain separatn, Å	8.136[b]	8.404[b]
	9.435[b]	9.311[b]
	10.969[c]	11.509[c]
	13.791[c]	13.491[c]

[a] <15 Å. [b] Out-of-registry. [c] In-registry.

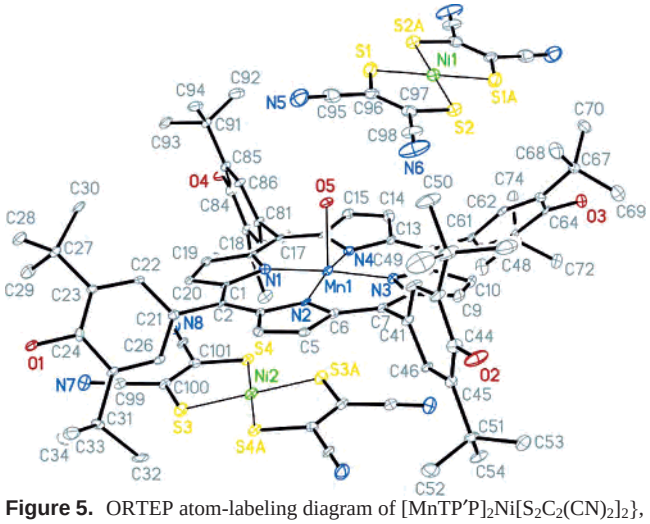

Figure 5. ORTEP atom-labeling diagram of [MnTP′P]$_2$Ni[S$_2$C$_2$(CN)$_2$]$_2$}, **6**, depicted without solvent molecules and with symmetry-completed Ni complexes using 30% thermal ellipsoids.

of χT for **3**−**5** are 2.55, 3.28, and 2.86 emuK/mol, respectively, averaging 2.90 emu K/mol, in accord with the expected value for and $S = 2$ and $S = 1/2$ spins of 3.38 emu K/mol, with antiferromagnetic coupling.[36] For **3** and **4**, the moment remains relatively constant with decreasing temperature until approximately 50−100 K (Figure 6). Above 20 K, $\chi T(T)$ can be fit to the Curie−Weiss expression, $\chi \propto 1/(T - \Theta)$, with $\Theta = -1.4$ and -0.57 K for **3** and **4**, respectively, indicating weak antiferromagnetic coupling. Above 190 K for **5**, $\chi T(T)$ changes slope; if data could be taken to a higher temperature, $\chi T(T)$ could be fit with $\Theta < 0$ K. $\chi T(T)$, however, is linear between 80 and 190 K and can be fit to the Curie−Weiss expression with effective Θ, Θ', of 49 K (Figure 6).

The [MnTPP][TCNE]·*x*S family of compounds has significant antiferromagnetic intrachain interactions and order as ferrimagnets. Minima in the $\chi T(T)$, T_{min}, are observed at 22 and 8 K for **3** and **4**, respectively, that indicate dominant antiferromagnetic coupling.[23] Typically, the $\chi T(T)$ data above ∼50 K can be fit to the Seiden expression[36] for a uniform isolated 1-D chain comprised of alternating quantum ($S = 1/2$) and classical ($g = 2$; $S = 2$) spin sites ($H = -2J\mathbf{S}_i\cdot\mathbf{S}_j$). However, below ∼50 K, the onset of long-range interchain coupling occurs and no appropriate magnetic model exists.

The 1-D intrachain coupling, J_{intra}, of **3**−**5** was determined from modeling $\chi T(T)$ by the Seiden expression with $J/k_B = -8.0$ K ($J = -5.6$ cm^{-1}) for **3**, -3.0 K (-2.1 cm^{-1}) for **4**, and -122 K (-85 cm^{-1}) for **5** (Figure 6). These observed negative J_{intra}/k_B values are indicative of antiferromagnetic coupling. The Seiden model is not valid below ∼50 K due to increased 3-D spin correlations or for systems in which the intrachain coupling is weak, likely due to next nearest neighbor interactions. For **5** the Seiden model was modified to include Θ, to account for the interchain interactions, and $\Theta = -8$ K (-5.6 cm^{-1}) indicating antiferromagnetic interchain couplings, which are much weaker than the intrachain interactions, i.e., -122 K.

Isothermal field-dependent magnetization, $M(H)$, experiments reveal magnetizations at 50 kOe and at 2 K of 10 700 (**3**), 15 000 (**4**), and 11 700 (**5**) emu Oe/mol. For an antiferromagnetic $S_{tot} = 2 - 1/2 = 3/2$ system, the expected saturation magnetization, M_s, is 16 755 emu Oe/mol, and for a ferromagnetic $S_{tot} = 2 + 1/2 = 5/2$ system, M_s is expected to be 27 925 emu Oe/mol. The magnitude of the magnetiza-

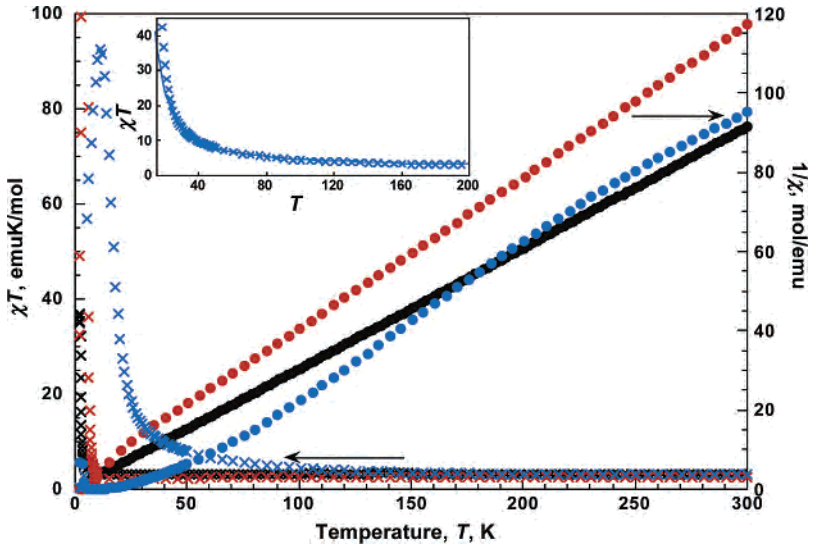

Figure 6. $\chi^{-1}(T)$ and $\chi T(T)$ for **3** (●, ×), **4** (●, ×), and **5** (●, ×). The inset shows the fit of $\chi T(T)$ to the Seiden model (see text) for **5**.

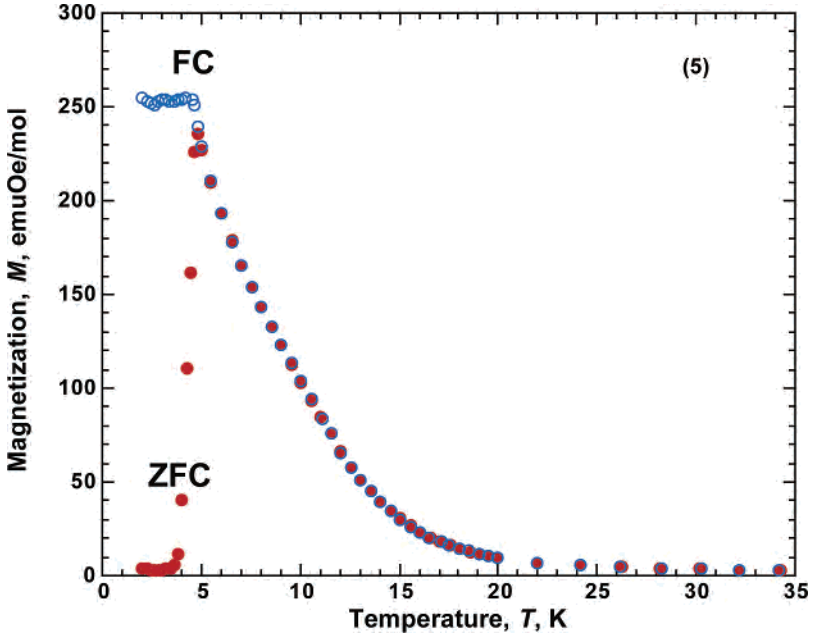

Figure 7. Zero field (ZFC) and field cooled (FC) $M(T)$ for **5**.

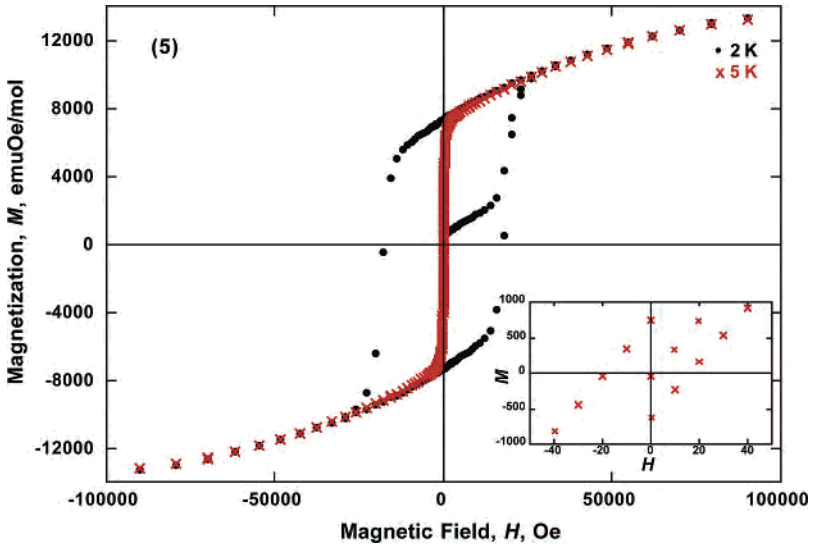

Figure 8. 2 K $M(H)$ showing hysteretic behavior for **5**.

tion at 5 T (and even 9 T of 13 300 emu Oe/mol for **5**) is lower than expected for an antiferromagnetically coupled $S_{tot} = 2 - 1/2$ system; however, on the basis of the slope of the $M(H)$ curves, saturation was not evident. Thus, these materials are ferrimagnets.[7b]

Magnetic ordering temperatures, T_c, were determined by the peak in the in-phase susceptibility at 10 Hz, $\chi'(T)$, and are from 5.5, 2.3, and 8.0 K for **3**−**5**, respectively. Both the in-phase and out-of-phase ac susceptibilities are frequency dependent. Frequency (ω) dependencies of the ac susceptibility, $\phi = \Delta T_f/(T_f\, \Delta(\log \omega)$, and are 0.015, 0.031, and 0.19 for **3**−**5**, respectively. The values for **3** and **4** are consistent with typical spin glasses[26] as reported for related materials.[4a,20] The higher value of 0.19 for **5** is characteristic of greater disorder, presumable due to the *tert*-butyl groups, as reported for [MnTP′P][TCNE]·2PhMe that has $\phi = 0.18$.[16] Very small ϕ values (<0.001) are typically noted for ferromagnets and weak ferromagnets. However, disordered spins systems display ϕ values which typically range from 0.01 to 0.1 such as found in the alloys of *Pd*Mn, $\phi = 0.013$, and *Ni*Mn, $\phi = 0.018$, and the superparamagnet α-$(Ho_2O_3)(B_2O_3)$, $\phi = 0.28$.[26]

Zero-field-cooled and field-cooled magnetic measurement were taken below 35 K at 5 Oe field for **5** (Figure 7). These data reveals a bifurcation temperature, T_b, at 4.8 K in accord with magnetic ordering.

Magnetic ordering is further evidenced by the presence of hysteresis loop that is observed for **3** and **5**. **3** exhibits a coercive field, H_{cr}, of 550 Oe and remanent magnetization of 7800 emu Oe/mol at 2 K. Due to the higher T_c, **5** has a H_{cr} of 17 700 Oe and remanent magnetization of 7250 emu Oe/mol at 2 K and 17 Oe and 850 emu Oe/mol at 5 K, respectively (Figures 8 and 9). Albeit large, the 2 K 17 700

(36) Seiden, J. *J. Phys. Lett.* **1983**, *44*, L947.

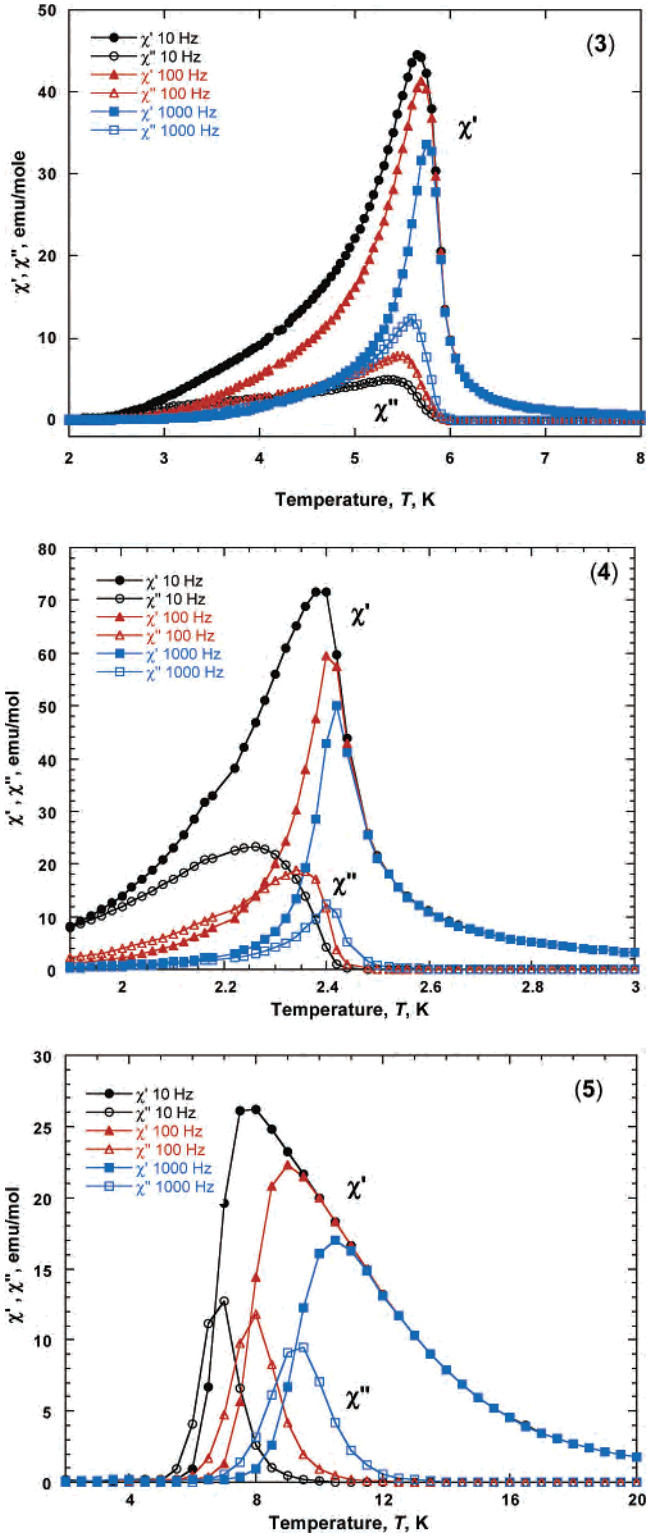

Figure 9. Real, $\chi'(T)$, and imaginary, $\chi''(T)$, ac susceptibilities for **5**. The lines are guides.

Oe coercivity is lower in value than that observed for the [MnTPP][TCNE] family of molecule-based magnets, which frequently have coercivities exceeding 25 000 Oe.[9] The 5 K H_{cr} values for the [MnTPP][TCNE] family of ferrimagnets are much smaller than that observed at 2 K and typical in the range of several hundred Oe. **5**, however, is atypical due to its 5 K H_{cr} 1 order of magnitude lower. Hence, upon cooling **5** goes from being a soft magnet to being a very hard magnet. The coercivity decreases linearly with increasing temperature, as observed for [MnTBrPP][TCNE] (MnTBrPP = (*meso*-tetrakis(4-bromophenyl)porphinato)manganese(III).[9]

In contrast, **4** does not exhibits either a H_{cr} or M_{rem} that is atypical for [Mn(porphyrin)][TCNE] systems[17] due to its low T_c with respect to the 2 K at which the measurements are made.

A relationship between structure and magnetic properties continues to be elusive. The data herein and that previously reported[3a,16] demonstrate a trend toward higher Θ' being associated with smaller dihedral angle formed from the $[TCNE]^{\bullet-}$ and MnN_4 mean planes. These angles are influenced by the size of the solvent molecule or porphyrin ring substituents.

MO Calculations. Mulliken and NBO charge and spin density calculations were performed using the B3LYP DFT and the 6-31++g(d,p) basis set for both $\{Ni[S_2C_2H(CN)]_2\}^{\bullet-}$ (**1**) and $\{Ni[S_2C_2(CN)_2]_2\}^{\bullet-}$ (**2**) (Table S1 and S2).

The Mulliken and NBO charge distributions for **1** and **2** differ significantly (Table S1 and S2). The Mulliken charge distribution reveals the majority of the positive charge for **1** resides on C1 and H, 0.20 and 0.21, respectively. However, for **2** the majority of the positive charge is on C1, 0.53, with Ni having 0.16 (vs 0.05 for **1**). This is at variance to the NBO charge distributions where the majority of the positive charge for both **1** and **2** reside on Ni (0.49 each). In addition the Mulliken charge distribution for **1** reveals a −0.11 charge difference between S1 and S2 and a −0.07 difference between C1 and C3, whereas the NBO charge distribution for **1** shows no difference between S1 and S2 and only a −0.01 difference between C1 and C3. Thus, the trans-substitution of H for CN caused a significant change in the Mulliken charge distribution but little to no effect in the NBO charge distribution.

The NBO spin distributions for **1** and **2** (Tables S1 and S2) reveal that the majority of the positive spin density/atom resides on Ni with values of 0.22 and 0.23, respectively. In addition the NBO spin distribution for **1** reveals a 0.06 spin density difference between S1 and S2 and a 0.03 difference between C1 and C3; similar differences are observed in the Mulliken spin distribution. In general the presence of H in **1** allows a small potion of the positive spin density present on Ni and S to be pulled further out onto the molecule, a possible explanation for why **3** has a higher T_c than **4**.

Acknowledgment. The authors gratefully acknowledge discussions with Israel Goldberg (Tel Aviv University) and support in part from the National Science Foundation Grant Nos. CHE9730948, CHE 0110685, and CHE-9002690.

Supporting Information Available: Calculated NBO and Mulliken charge and spin (α and β) distributions as well as total electron populations for $\{Ni[S_2C_2H(CN)]_2\}^{\bullet-}$, **1**, and $\{Ni[S_2C_2(CN)_2]_2\}^{\bullet-}$, **2**. This material is available free of charge via the Internet at http://pubs.acs.org. X-ray CIF files for [MnTPP]$\{Ni[S_2C_2H(CN)]_2\}$, **3**, [MnTPP]$\{Ni[S_2C_2(CN)_2]_2\}$, **4**, and **6** have been deposited with the Cambridge Crystallographic Data Center, reference nos. CCDC-275193, CCDC 275194, and CCDC 275195, respectively.

IC050980U